A Shift of Phloem Unloading from Symplasmic to Apoplasmic Pathway Is Involved in Developmental Onset of Ripening in Grape Berry[1]

Xiao-Yan Zhang[2], Xiu-Ling Wang[2], Xiao-Fang Wang[2], Guo-Hai Xia, Qiu-Hong Pan, Ren-Chun Fan, Fu-Qing Wu, Xiang-Chun Yu, and Da-Peng Zhang*

China State Key Laboratory of Plant Physiology and Biochemistry, China Agricultural University, 100094 Beijing, China

It remains unclear whether the phloem unloading pathway alters to adapt to developmental transition in fleshy fruits that accumulate high level of soluble sugars. Using a combination of electron microscopy, transport of the phloem-mobile symplasmic tracer carboxyfluorescein, movement of the companion cell-expressed and the green fluorescent protein-tagged viral movement protein, and assays of the sucrose cleavage enzymes, the pathway of phloem unloading was studied in the berries of a hybrid grape (*Vitis vinifera* × *Vitis labrusca*). Structural investigations showed that the sieve element-companion cell complex is apparently symplasmically connected through plasmodesmata with surrounding parenchyma cells throughout fruit development, though a small portion of plasmodesmata are apparently blocked in the ripening stage. Both carboxyfluorescein and the green fluorescent protein-tagged viral movement protein were released from the functional phloem strands during the early and middle stages of fruit development, whereas the two symplasmic tracers were confined to the phloem strands during the late stage. This reveals a shift of phloem unloading from symplasmic to apoplasmic pathway during fruit development. The turning point of the phloem unloading pathways was further shown to be at or just before onset of ripening, an important developmental checkpoint of grape berry. In addition, the levels of both the expression and activities of cell wall acid invertase increased around the onset of ripening and reached a high level in the late stage, providing further evidence for an operation of the apoplasmic unloading pathway after onset of ripening. These data demonstrate clearly the occurrence of an adaptive shift of phloem unloading pathway to developmental transition from growing phase to ripening in grape berry.

The phenomenon of phloem unloading has been studied extensively over the last 20 years (Oparka, 1990; Patrick, 1997; Viola et al., 2001) but still remains poorly understood. Phloem unloading is believed to play a key role in the partitioning of photoassimilates, so determining to a large extent crop output (Fisher and Oparka, 1996; Patrick, 1997). The unloading pathway is a central process of the unloading mechanism to determine the key transport events responsible for assimilate movement from the sieve elements (SEs) to the recipient sink cells (Fisher and Oparka, 1996; Patrick, 1997). Evidence from several plant species suggests that a symplasmic pathway predominates in most sink tissues, although transfer of solutes to the apoplast may occur at some point along the post-phloem pathway (Patrick, 1997; Roberts et al., 1997; Imlau et al., 1999; Oparka and Santa Cruz, 2000; Haupt et al., 2001; Viola et al., 2001; van Bel, 2003). The predominance of the symplasmic unloading pathway has been considered to be associated with greater transport capacity and lower resistance (Patrick and Offler, 1996; Patrick, 1997; van Bel, 2003).

However, several studies revealed that the phloem unloading routes are changeable, and may shift in response to sink development and function. Roberts et al. (1997) revealed that symplasmic phloem unloading pathway may be blocked during sink-to-source transition in tobacco (*Nicotiana tabacum*) leaves. Viola et al. (2001) found that tuberization of potato (*Solanum tuberosum*) stolons is associated with a switch from apoplasmic to symplasmic phloem unloading pathway. The modification of the phloem unloading pathway may result from changes in the numbers or conductivity of plasmodesmata, and this modification due to plasmodesmal regulation has been believed to be of special importance to sink development and function (Patrick, 1997; Oparka and Turgeon, 1999; van Bel, 2003).

Plasmodesmal function in developmental transition of various plant tissues has been studied extensively in recent years. Oparka et al. (1999) revealed a decrease in the permeability of leaf mesophyll plasmodesmata when leaves underwent the sink/source transition. Gisel et al. (1999, 2002) demonstrated a transition from symplasmic connection with surrounding cells to

[1] This work was supported by the grants from China National Natural Science Foundation (grant nos. 30421002, 30330420, and 30471193 to D.-P.Z.), the National Key Basic Research Program of China (grant no. 2003CB114302 to D.-P.Z.), and a "948" Research Program from the China Ministry of Agriculture (to D.-P.Z).

[2] These authors contributed equally to the paper.

* Corresponding author; e-mail zhangdp@sohu.net; fax 86–10–62731899.

The author responsible for distribution of materials integral to the findings presented in this article in accordance with the policy described in the Instruction for Authors (www.plantphysiol.org) is: Da-Peng Zhang (zhangdp@sohu.net).

www.plantphysiol.org/cgi/doi/10.1104/pp.106.081430

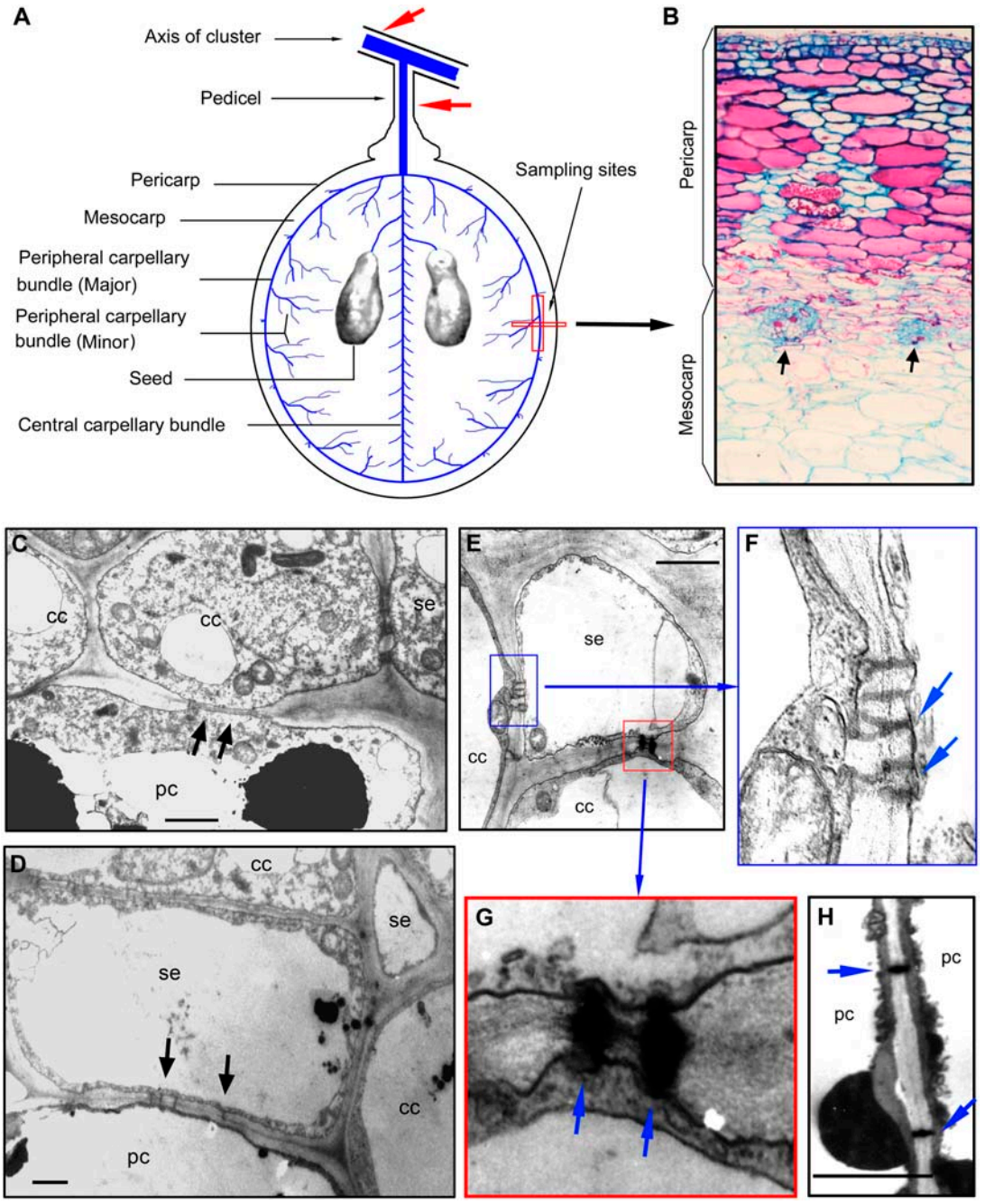

Figure 1. Structure of grape berry. A, Longitudinal section of a grape berry, showing the network of the vascular bundles, the loading site of CFDA into the axis of the cluster or the pedicel (indicated by red arrows), the sampling sites for structural observations, immunolabeling of acid invertases, and the CF transport imaging shown in Figure 2. B, Anatomical section of pericarp and mesocarp of grape berry. Arrows indicate the peripheral carpellary bundles. C, A transverse section of the phloem in the peripheral carpellary bundle at the beginning of developmental Stage I (10 d after anthesis). Arrows indicate plasmodesmata between CC and PC. D, A transverse section of the phloem in the peripheral carpellary bundle at the beginning of developmental Stage III. Arrows indicate plasmodesmata between SE and PC. E, SE-CC complexes in the peripheral carpellary bundle, showing two different classes of plasmodesmata between SE and CC (boxed-in areas), one being apparently normal and with branched channels as shown more clearly in the blow-up (F; arrows indicate the branched channels), and the other blocked by the electron-opaque globules (blow-up shown in G). H, A picture showing the electron-opaque globule-blocked plasmodesmata (arrows) between two PCs. Berries for ultrastructural observations in E to H were sampled at the beginning of developmental Stage III (see Fig. 2). Bars = 1 μm in C to E, and H. Abbreviations: cc, companion cell; pc, parenchyma cell; se, sieve element.

symplasmic isolation of Arabidopsis (*Arabidopsis thaliana*) inflorescence meristems before flowering initiation. Ruan et al. (2001, 2004) found a similar phenomenon in cotton (*Gossypium hirsutum*) fibers during rapid elongation of the fibers. The domain of symplasmic isolation was also shown to be formed during embryogenesis in Arabidopsis (Kim et al., 2002). Itaya et al. (2002) demonstrated that selective intercellular protein trafficking within or between the symplasmic domains may be realized, which may allow possible communication of developmental signals between these tissues.

In contrast to this, however, little attention has been given to plasmodesmal regulation in the adaptation of phloem unloading pathways to the functions of economically important sink organs. To our knowledge, in addition to starch-storing potato tubers (Viola et al., 2001), only tomato (*Lycopersicon esculentum*) fruit that accumulates low level of soluble sugars was shown to operate a symplasmic post-phloem unloading at the early stages but an apoplasmic post-phloem unloading during the late stages (Ruan and Patrick, 1995), but it has been unclear whether the unloading pathway of the SE-companion cell (CC) complex changes during tomato fruit development.

Fleshy fruits are one class of terminal reproductive strong storage sinks, but the mechanism of phloem unloading has received little attention in comparison to vegetative sinks and developing seeds (Oparka, 1990; Patrick, 1997). In the fleshy fruits that, unlike tomato fruit, accumulate high concentrations of soluble sugars, apple (*Malus domestica*) fruit was shown to follow an extensive apoplasmic phloem unloading pathway (Zhang et al., 2004). In citrus fruit, disruption of the symplasmic continuity within the stalks of juice vesicles and [^{14}C]assimilate tracing suggest an apoplasmic post-phloem transport (Koch and Avigne, 1990).

Grape (*Vitis vinifera*) berry is one of the economically important sink organs in which sugar accumulation is a major determinant of yield and quality, but the phloem unloading pathway in this berry fruit remains largely unknown. A previous report suggested an apoplasmic mode of phloem unloading by showing in the berry apoplast the occurrence of a high level of sugars that was sensitive to changes in the rate of phloem import (Brown and Coombe, 1985). Here, we report that a symplasmic unloading pathway predominates in the early and middle stages, but an apoplasmic unloading pathway operates in the ripening stage during fruit development, and that a shift of phloem unloading from symplasmic to apoplasmic pathway is involved in developmental onset of ripening of grape berry.

RESULTS

Structurally, the SE-CC Complex Is Symplasmically Connected to Surrounding Cells

Grape berry is a typical true fruit originating from ovary. The fleshy portion comes from the ovary wall that gives the pericarp, mesocarp, and endocarp (Fig. 1, A and B). The mesocarp is the main edible berry flesh (Fig. 1, A and B). Therefore, the developing grape berry is fed with photoassimilates through the carpellary vascular bundles that are divided into the peripheral and central bundles (Fig. 1, A and B). Our previous investigation that concerned only the major carpellary bundle showed that the plasmodesmatal densities (Kempers et al., 1998; van Bel, 2003) between the SE-CC complex and its adjacent cells was low at the early stage of berry development (Xia and Zhang, 2000). A detailed examination in this study shows that, in both the major and minor carpellary bundles, a potential symplasmic connection through plasmodesmata exists between the SE-CC complex and surrounding parenchyma cells (PCs), and also between two adjacent PCs (Fig. 1, C and D; Table I). There are more plasmodesmata at the interface between SE and CC than between SE-CC complex and PCs or between adjacent PCs (Fig. 1, C and D; Table I). This holds true throughout berry development (Table I). However, we observed during the late stage that some plasmodesmal channels (approximately 10%–20%; Table I) are apparently blocked by electron-opaque globules in the interfaces between SE and CC, or SE-CC complex and PCs and also between two PCs (Fig. 1, E, G, and H; Table I), and a small portion (about 5%) of plasmodesmata channels are branched (Fig. 1F). Nevertheless, most of plasmodesmata (approximately 70%) remain apparently normal (Table I), i.e. neither branched nor blocked by the electron-opaque material or callose (van Bel, 2003).

Before Ripening, CF and 3a MP:GFP Escape from, But after Ripening Are Confined to, Phloem Strands

When it is loaded into cells, the membrane-permeable and nonfluorescent 6(5) carboxyfluorescein diacetate (CFDA) is degraded to 6(5) carboxyfluorescein (CF), a membrane-impermeable fluorescent dye. CF is often used as a fluorescent marker of phloem transport and symplasmic phloem unloading (Roberts et al., 1997; Viola et al., 2001). Our preliminary experiments showed that CF supplied to the axis of cluster or directly to

Table I. *Plasmodesmal densities between different cells in phloem of the major and minor peripheral carpellary bundles of grape berry during the developmental Stages I to III*

Unit of plasmodesmal densities, number of plasmodesmata μm^{-1}. Values in parentheses represent the density of plasmodesmata blocked by electron-opaque material.

Stage	Bundle	SE/CC	SE/PC	CC/PC	PC/PC
I	Major	2.01	1.21	0.80	0.42
	Minor	2.13	1.15	0.75	0.39
II	Major	2.02	1.15	0.77	0.40
	Minor	2.07	1.20	0.81	0.41
III	Major	2.21 (0.5)	1.08 (0.2)	0.76 (0.1)	0.40 (0.1)
	Minor	2.09 (0.4)	1.19 (0.3)	0.77 (0.1)	0.38 (0.1)

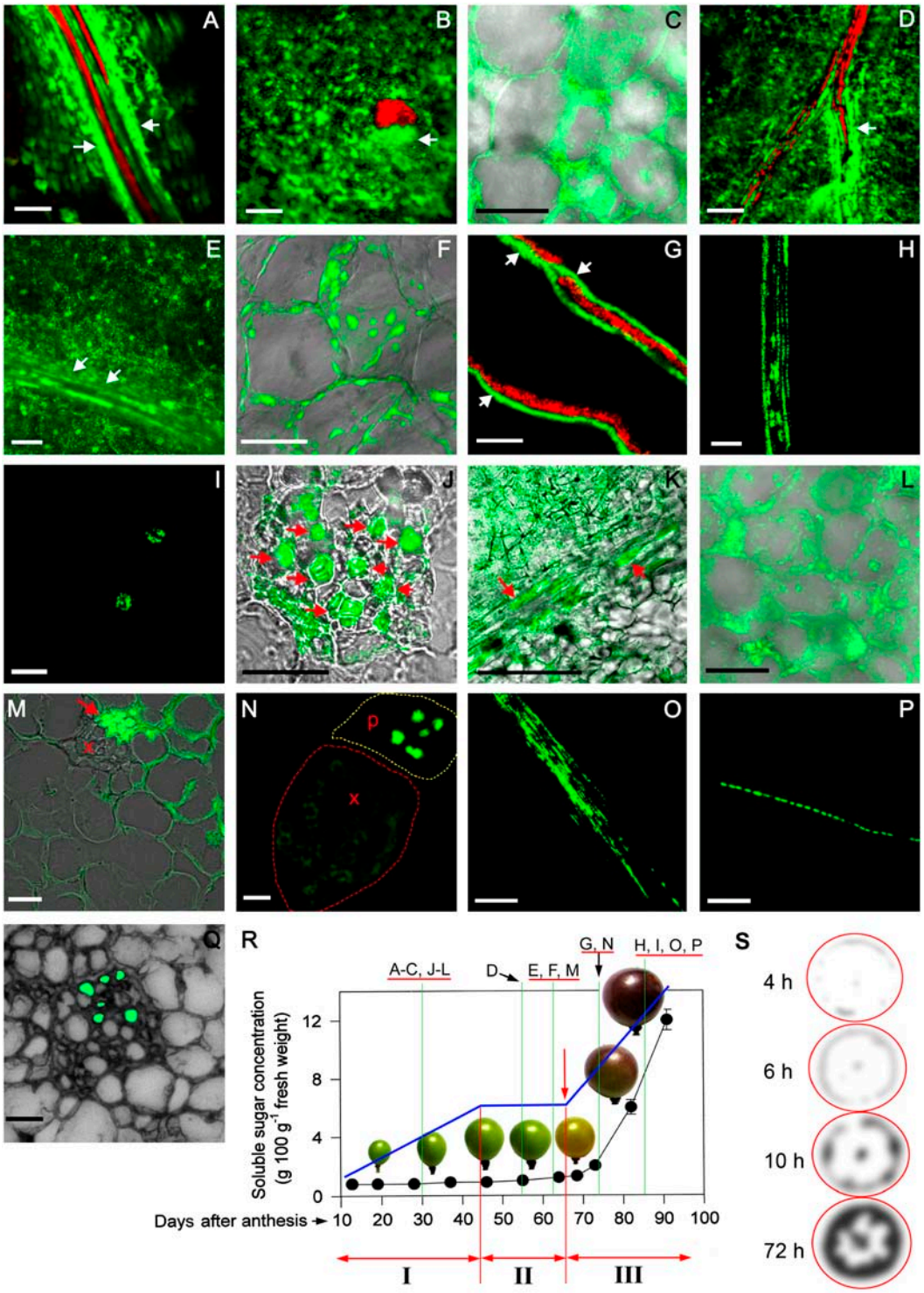

Figure 2. CLSM imaging of CF (A–I) and 3a MP:GFP (J–P) unloading during development of grape berry. The sampling time is indicated in R. CF reached the berry phloem 3 to 4 h after loading of the pedicel or axis of the cluster (see Fig. 1A). The treated berry was sampled 72 h after CF loading and the sections by free hand or freezing microtome were prepared from the peripheral carpellary bundle zone (indicated in Fig. 1A). The red strands in A, D, and G and red area in B indicate the xylem zones labeled by Texas Red dextran. A to C, Berries collected in the middle of Stage I (around 30 d after anthesis). The green fluorescence of CF was shown to be released from the phloem strands (indicated by arrows) in longitudinal (A) and transverse (B) sections of the zones of the major peripheral carpellary bundle. C, Distribution of CF in PCs (a section by freezing microtome). D, Berries collected in the middle of Stage II (around 55 d after anthesis), showing release of CF from the phloem strands (indicated by arrow) of the branched minor peripheral carpellary bundle (see Fig. 1A). E and F, Berries collected in late Stage II (around 65 d

berry pedicel reached the berry flesh 3 to 4 h after CF loading, which is in good agreement with the transport velocity of [^{14}C]Suc (see Fig. 2S). Confocal laser scanning microscopy (CLSM) images of CF movement in the berries sampled 72 h after CF supply to the pedicel are presented in Figure 2. A series of experiments conducted during berry development showed that CF was released from the phloem strands along the phloem pathway at the early developmental stage (Fig. 2, A and B) and the middle stage (Fig. 2, D and E), i.e. the first rapid growth stage (Stage I) and lag stage of growth (Stage II; see Fig. 2R) before ripening, as shown in both the major (Fig. 2, A, B, and E) and minor (Fig. 2D) peripheral carpellary bundles. CF was shown to distribute in PCs during Stages I (Fig. 2C) and II (Fig. 2F). During the developmental Stage III, i.e. the second rapid growth phase or ripening stage (see Fig. 2R), however, CF was confined to the phloem strands of the peripheral carpellary bundles without apparent release, as shown in longitudinal (Fig. 2, G and H) and transverse (Fig. 2I) sections.

To confirm the above CF unloading pathways, we used a green fluorescent protein (GFP)-tagged movement protein 3a MP of the *Cucumber mosaic virus* whose expression is controlled by the CC-specific promoter of *Commelina yellow mottle virus* (CoYMV; Matsuda et al., 2002). The CC-expressed fusion protein 3a MP:GFP (57 kD) was previously shown to be able to efficiently pass through plasmodesmata even between symplasmically isolated cells due to reduced plasmodesmal channels (Itaya et al., 2002). The 3a MP:GFP was shown by CLSM imaging to be specifically expressed in the CCs of grape berry (Fig. 2J). This fusion protein spread from the phloem strands of the peripheral carpellary bundles to surrounding PCs during developmental Stages I and II before ripening (Fig. 2, J–M), but was restricted to the phloem strands without apparent release at Stage III during the ripening process (Fig. 2, N–P). We also used a dimeric GFP fusion protein (GFP:GFP fusion; 54 kD) under the control of the CoYMV promoter (Itaya et al., 2002) to generate transgenic berry tissue, and observed by CLSM no apparent release of the dimeric GFP from the CCs of the berry phloem (Fig. 2Q), indicating that the 3a MP:GFP transport observed in the berry tissue is a trafficking process specifically through plasmodesmata but not a phenomenon of simple diffusion. Thus, the 3a MP:GFP imaging supports the above observations of CF transport.

The Turning Point of CF and 3a MP:GFP Unloading Pathway Is at Onset of Ripening

We gave particular attention to the turning time of the CF and 3a MP:GFP unloading pathway. The investigations around the ripening date, i.e. 6 to 4 d before (Fig. 2, E and F, for CF; Fig. 2M for 3a MP:GFP transport) and 4 to 6 d after (Fig. 2G for CF; Fig. 2N for 3a MP:GFP transport) onset of ripening, suggest that the turning point may be around the onset of ripening.

To further test this turning time, we took a survey of CF unloading in the whole berry by serial sections observed under fluorescence microscope. On the sections at the pedicel side (Fig. 3B, a; see also Fig. 3A, a), middle (Fig. 3B, b), top (Fig. 3B, c; see also Fig. 3A, b), and lateral (Fig. 3B, d) zones of whole berry, CF

Figure 2. (*Continued*).
after anthesis or 4–6 d before the onset of ripening). CF was shown to be released from phloem (indicated by arrows) in a longitudinal section of the major peripheral carpellary bundle (E) and to spread in PCs (F, a section by freezing microtome). G to I, Berries collected at the early (about 6 d after the onset of ripening; G) and the middle of Stage III (about 20 d after the onset of ripening; H and I). CF was confined to the phloem zones of the peripheral carpellary bundles in longitudinal (G and H, with arrows indicating phloem strands in G) and transverse (I) sections. J to L, Berries collected in the middle of Stage I (around 30 d after anthesis). J, The expression of 3a MP:GFP was clearly observed in CCs (indicated by red arrows) of the phloem of a minor peripheral carpellary bundle 15 h after the coincubation of berry tissue with *CoYMV:3a MP:GFP*-carrying *Agrobacterium tumefaciens* and began to spread to the surrounding cells (J, a section by freezing microtome). K, Release of 3a MP:GFP from the phloem zone (indicated by arrows) in a major peripheral carpellary bundle 20 h after the coincubation. L, Distribution of 3a MP:GFP in the PCs (a section by freezing microtome). M, Berries collected in the late Stage II (around 65 d after anthesis or 4–6 d before the onset of ripening). 3a MP:GFP spread from the phloem (indicated by arrow) of a minor peripheral carpellary bundle to surrounding PCs (a section by freezing microtome). "x" denotes xylem zone. N to P, Berries collected at the early (about 6 d after the onset of ripening, N) and the middle Stage III (about 20 d after the onset of ripening, O and P), showing that 3a MP:GFP was confined to the phloem zones of the peripheral carpellary bundles. N, A transverse section of a peripheral vascular strand. Phloem zone (p) is outlined by dotted yellow line and xylem (x) by dotted red line. Weak autofluorescence of xylem vessels can be seen in the xylem zone. O and P, Longitudinal sections of the major peripheral carpellary bundles. Q, The dimeric GFP fusion protein was expressed in and confined to CCs in phloem. R, A schema showing the developmental stages of grape berry and sampling time (the underlined letters A–P above the schema) in the above-described experiments. Berry growth (in volume) is expressed in relative data (%). The developmental Stage I represents the first rapid growth phase, Stage II the lag phase of growth, and Stage III the second rapid growth phase or ripening phase. The red arrow denotes the transition from Stage II to Stage III, i.e. onset of ripening. S, Time course of ^{14}C-Suc transport from the loading sites in the pedicel phloem to berry tissues. ^{14}C-Suc was fed to the pedicel in the same manner as CF was, and the ^{14}C-Suc distribution in berries was detected by ^{14}C-autoradiography at the indicated times (4, 6, 10, and 72 h after the ^{14}C-Suc loading). Red circles indicate berry outlines. Bars = 100 μm in A to C, E, G, H, I, K, O, and P. Bars = 10 μm in D, F, J, L to N, and Q. Each value presented in R for soluble sugar concentrations is the mean of five replicates ± SD.

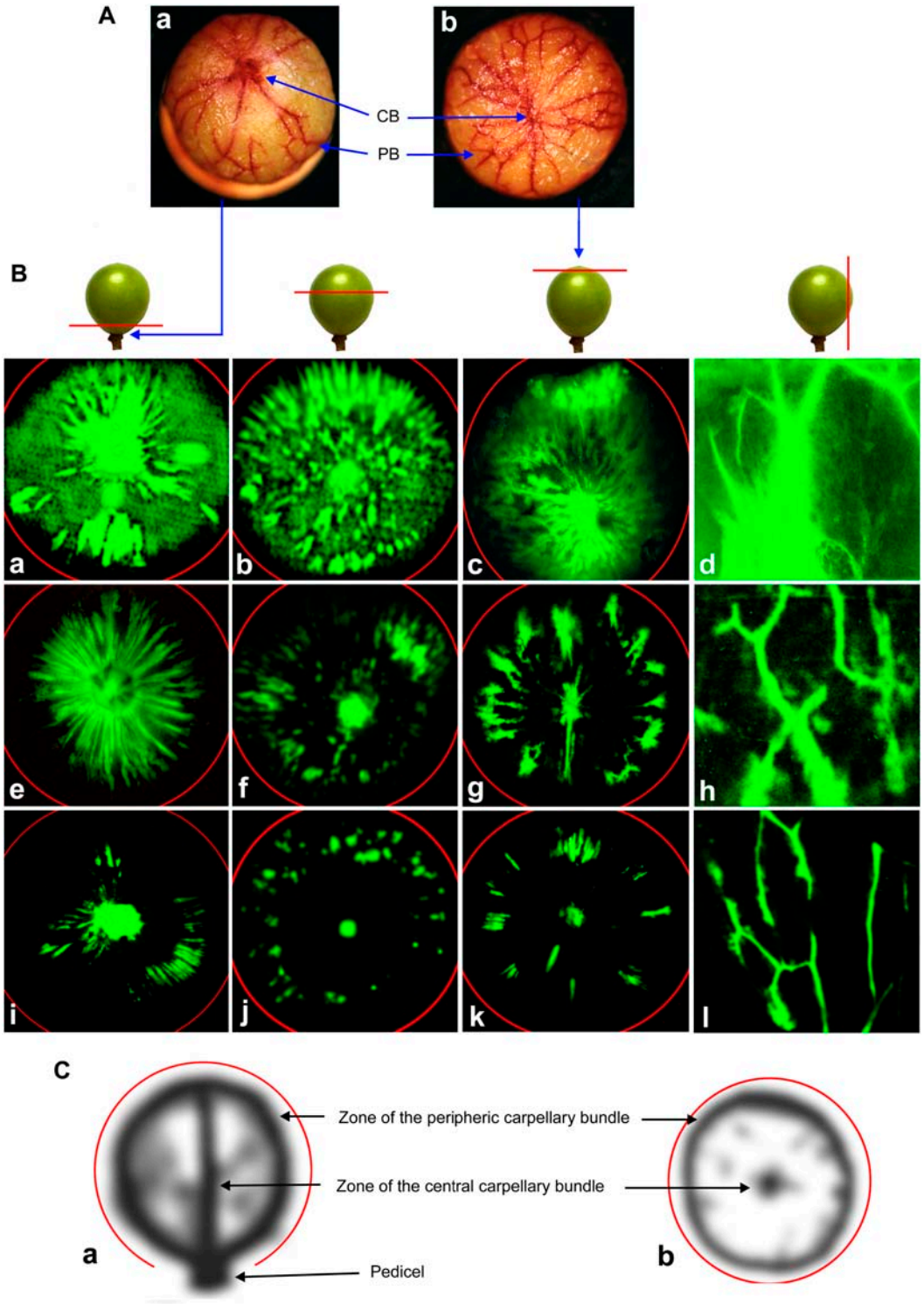

Figure 3. CF transport imaging in whole berry around the onset of ripening and ^{14}C-labeling of vascular bundles. A, For better guiding the observations of CF and ^{14}C-assimilate transport, the vascular bundles were labeled by allowing berry to transpire safranine dye. A view at the pedicel side (a) and another view at the berry top side (b) show the network of the peripheral carpellary bundle (PB) and the position of the central carpellary bundle (CB). B, CF transport in whole berry. The red lines marked on berry models indicate the sectioning sites for the corresponding columns of the panels below the models. Berries were allowed to transport CF for 72 h, and then were collected and sectioned by free hand for observations under a fluorescence microscope. B, a to d, Berries treated by CFDA 6 d before onset of ripening. CF spread all over the berry from both the peripheral and central carpellary bundles (see A above and Fig. 1A for the network of the bundles). B, e to h, Berries treated by CFDA 1 d after onset of ripening. CF apparently spread, but to a much more reduced extent than before onset of ripening (see a–d). B, i to l, Berries treated by CFDA 4 d after onset of ripening. CF was restricted to both the peripheral and central carpellary bundles. C, ^{14}C autoradiography in the middle of Stage II. ^{14}C-labeled assimilates were transported in both the peripheral and central carpellary bundles, which are shown in longitudinal (a) and transverse (b) sections. Red circles in B and C indicate the outlines of the grape berry.

was shown to be intensively released from both the peripheral and central carpellary bundles 6 to 4 d before the onset of ripening, but this CF release was largely reduced 1 to 3 d after the onset of ripening on these whole berry sections (Fig. 3B, e–h). CF was substantially confined to the peripheral and central carpellary bundles 4 to 6 d after the onset of ripening (Fig. 3B, i–l). These data further confirm the above observations of CLSM imaging of CF and 3a MP:GFP transport in both the peripheral and central carpellary bundles of whole grape berry, and demonstrate that the turning point of the phloem unloading pathway is at the onset of ripening.

After feeding $^{14}CO_2$ to the leaves, [^{14}C]assimilates were apparently unloaded from the peripheral and central carpellary bundles to grape berry (Fig. 3C), revealing that the phloem of these bundles was functional for unloading.

Both the Activities of Cell Wall Acid Invertase and Levels of Apoplasmic Soluble Sugars Increase at Onset of Ripening

The activity of soluble acid invertases (SAIs) was previously reported to decrease from the onset of grape berry ripening (Davies and Robinson, 1996). We previously confirmed this finding and also observed an increase of acid invertase activity in the cell wall fractions in parallel with the decrease of soluble invertase activity in the ripening process (Pan et al., 2005b). A detailed study in this experiment showed that the cell wall invertase activity began to increase just before or around the onset of ripening, and then rapidly reached a high level at the onset of ripening, whereas the soluble invertase activity dropped to the lowest level at the onset of ripening (Fig. 4, A and B). The immunoblot-estimated amounts of both the cell wall and soluble invertases changed substantially in parallel with their activities (Fig. 4, A and B). An immunogold labeling assay showed clearly that acid invertases (visualized by immunogold particles) localize predominantly in vacuoles of both CC and PC before onset of ripening (Fig. 4, C and D), but they reside in cell walls of SE-CC complex and PC after the onset of ripening (Fig. 4, E and F). Importantly, no gold particles were substantially found in any of the controls without the antiserum or with the preimmune serum controls (data not shown), indicating that the antiserum was specific and that unspecific labeling was negligible.

Further investigations showed that the Suc synthase activities increased slightly during berry development but were not significantly correlated with soluble sugar concentrations (Fig. 4A). It is interesting to observe that the concentrations of total soluble sugars remained substantially constant in the phloem sap of pedicel during berry development but increased in the apoplasmic space of berry flesh after the onset of ripening (Fig. 4A).

DISCUSSION

Onset of Ripening Involves a Shift of Phloem Unloading from Symplasmic to Apoplasmic Pathway

The growth of grape berry follows a typical sigmoid growth curve with a lag phase of growth between two rapid growth phases. During the first rapid growth phase (Stage I) and lag phase of growth (Stage II), low levels of soluble sugars accumulate in the berries (see Fig. 4A). Following the lagging Stage II, the second rapid growth phase (Stage III) is characterized by a rapid increase of both the berry volume and soluble sugar accumulation with a rapid decrease of organic acid contents. The fruit ripens during Stage III, when nearly the totality of storage assimilates accumulates and fruit quality and yield are determined (Coombe, 1992; see also Figs. 2R and 4A). Thus, the transition from Stage II to Stage III involves complex processes to trigger the shift from lagging growth to spurring ripening. This period of the onset of ripening, transient in 1 to 2 d, has been considered to be a critical developmental checkpoint of grape berry.

We show in this study the occurrence of a shift of phloem unloading from symplasmic to apoplasmic pathway during this transient onset of ripening of grape berry. The cytological studies revealed that SE-CC complexes in the phloem of the peripheral vascular bundles that feed the berry flesh (mesocarp) are symplasmically connected with their surrounding PCs through plasmodesmal channels during fruit development (Fig. 1; Table I). An in vivo functional investigation by real-time imaging of movement of both the CF dye and viral 3a MP:GFP showed that the fluorescence escapes from the functional phloem of the carpellary bundles through the plasmodesmata-mediated symplasmic routes during Stages I and II (Figs. 2 and 3). This demonstrates that grape berry follows a predominant symplasmic phloem unloading pathway during the early and middle developmental stages. The distribution of the fluorescence of both CF and 3a MP:GFP in the storage PCs (Fig. 2) also revealed a symplasmic post-phloem unloading during these stages. However, the movement of these two symplasmic tracers was blocked during Stage III (Figs. 2 and 3), revealing that an apoplasmic pathway dominates during this late and ripening developmental process. A detailed survey of CF and 3a MP:GFP transport around the onset of ripening provides clear evidence that the turning time of the phloem unloading pathway is at or just before the onset of ripening (Figs. 2 and 3).

The pattern of the changes in the expression and activities of acid invertases during berry development (Fig. 4) supports the shift of phloem unloading pathway at the onset of ripening. As a matter of fact, acid invertase, which converts Suc into Glc and Fru, presents in the plant cell wall as insoluble form or in the vacuole as soluble form (Quick and Schaffer, 1996). It is believed that the continuous hydrolysis of Suc by acid

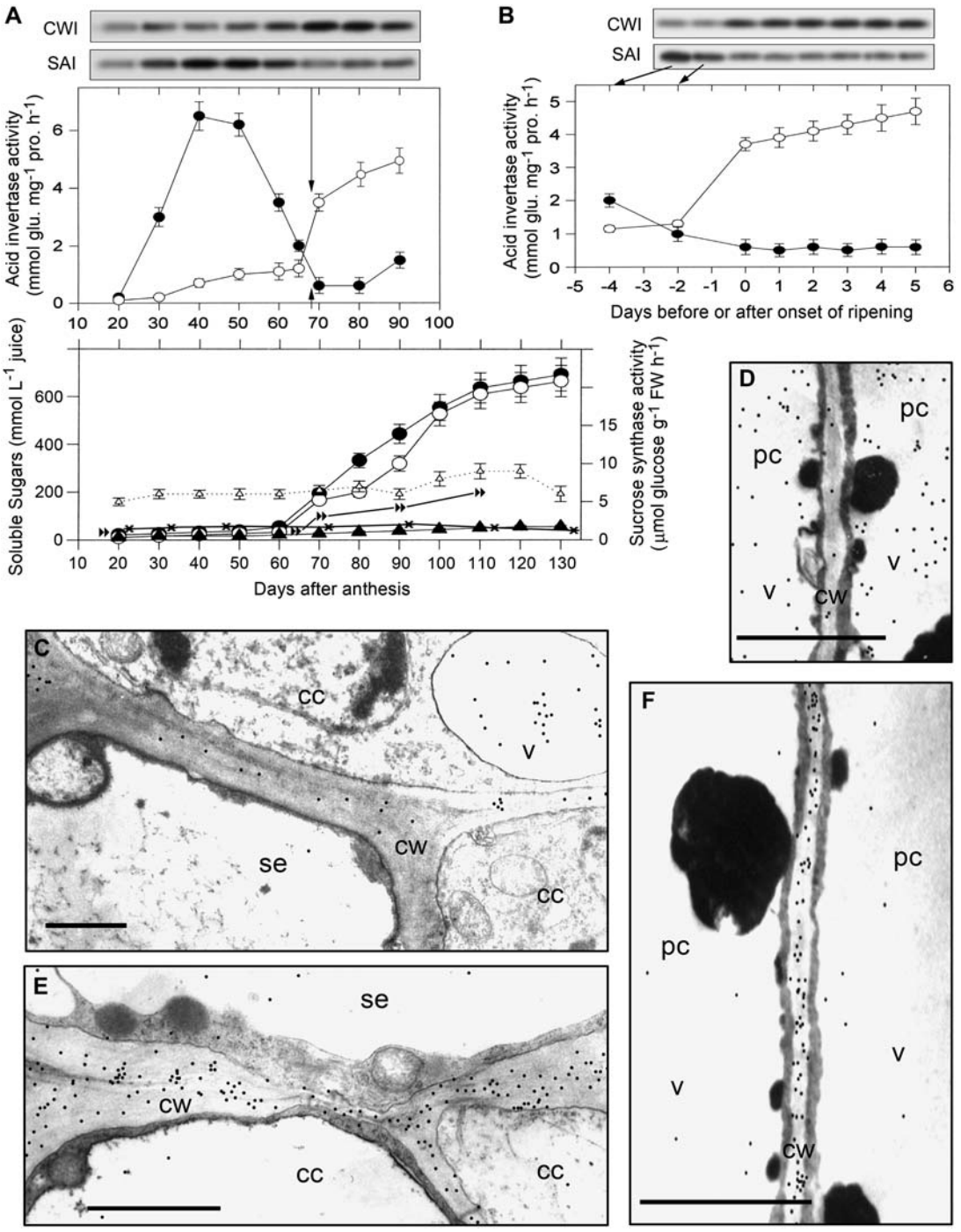

Figure 4. Changes in the acid invertase amounts and activities and Suc synthase activities as well as soluble sugar concentrations during berry development. The amounts of acid invertases were assessed by immunoblotting (A and B) and by immunogold labeling (C–F) with the antisera directed against apple fruit acid invertases. A, For cell wall acid invertase, the amounts (CWI, top) and activities (white circles, middle) increased slowly from the early stage and maintained at a low level during the middle stage, and then increased rapidly around the onset of ripening and reached a high level in the late stage. The amounts (SAI, top) and activities (black circles, middle) of SAI changed substantially in an inverse pattern compared to cell wall invertase. Arrows in the middle section indicate the onset of ripening. The bottom section in A displays the changes in the Suc synthase activities in the cleavage direction (white triangles), the concentrations of Fru (black circles), Glc (white circles), and Suc (black triangles) in berry flesh, and total soluble sugars in the phloem exudates (black asterisks) and in the apoplasmic space of berries (black double triangles). B, The onset of ripening was shown to be the turning point of the increase of cell wall invertase amounts (CWI, section above) and activities (white circles, section below). The amounts (SAI, section above) and activities (black circles, section below) of SAI substantially changed inversely compared to cell wall invertase. The day "0" denotes the date of the onset of ripening and

invertase at the unloading site increases the steepness of Suc gradient, leading to a faster unloading of Suc from the SE-CC complex, and so the presence of acid invertase in cell wall favors apoplasmic Suc unloading (Frommer and Sonnewald, 1995; Patrick, 1997). In this study, a rapid increase of cell wall invertase in both its amounts and activities from the onset of ripening was observed (Fig. 4). This presence of acid invertase in cell walls provides possible machinery to degrade Suc unloaded from phloem to the berry apoplast. Thus, in the apoplasmic space of berries, hexoses (Glc and Fru) derived from the Suc breaking may be loaded into the storage PCs via a trans-membrane pathway. Contrarily, the symplasmic phloem unloading seems to depend more on SAI than on cell wall invertase in grape berry. The Suc symplasmically imported from phloem into PCs can be hydrolyzed by the vacuole-localized invertase, which may explain the apparent correlation of SAI with symplasmic phloem unloading pathways during fruit development (Fig. 4). Suc synthase is another enzyme cleaving Suc into Fru and Glc, which, localized in both cytoplasm and plasma membrane, is believed to be associated with symplasmic unloading (for review, see Quick and Schaffer, 1996). The activities of Suc synthase remained substantially constant during berry development, though a slight increase occurred late in the ripening stage (Fig. 4A). This suggests that Suc synthase may cooperate with the vacuole invertase in cleaving the symplasmically unloaded Suc in storage PCs.

Taken together, these findings indicate that the developmental process of the onset of ripening is associated closely with the induction of symplasmic isolation between the SE-CC complexes and the PCs, forming an apoplasmic trans-membrane pathway of higher resistance to photoassimilate import during the ripening process.

Possible Mechanism and Significance of the Shift of Phloem Unloading Pathway

The decline in the transport capacity of the symplasmic channels should be responsible for the shift of phloem unloading from symplasmic to apoplasmic pathway. This decline may be attributed partly to the presence of the unknown electron-opaque material in the plasmodesmal pores at the interfaces between SE and CC, between SE-CC complex and CCs, and between adjacent CCs (Fig. 1; Table I). The branched plasmodesmata (Fig. 1) were also reported to be associated with low conductivity (Oparka et al., 1999). We also observed the presence of callose in plasmodesmal pores at the interface between SE and CC as shown by Vignault et al. (2005), but not between SE-CC complex and PCs (data not shown). The callose deposition may cause plasmodesmal closure (van Bel, 2003; Ruan et al., 2004). However, the plasmodesmal density remained unchanged during fruit development, and most of plasmodesmata (about 70%) appeared normal in the ripening stage (Fig. 1; Table I). These data suggest that a decrease in the plasmodesmal conductivity, but not in their numbers, may cause the shift of the unloading route at or just before the onset of ripening.

The shift of plasmodesmal conductivity is coordinated with the expression of solute transporters and cell wall-loosening gene during the transition of growth phases in cotton fibers, suggesting that an integration of plasmodesmal gating and gene expression may control cell elongation of cotton fibers (Ruan et al., 2001). Similarly to this, the coordinated shift of acid invertase expression with the phloem unloading pathway (Figs. 2–4) suggests that complex developmentally regulated processes, including, among others, decline of plasmodesmal conductivity and creation of an apoplasmic Suc cleaving machinery (i.e. cell wall invertase), are involved in developmental onset of grape ripening.

Why does grape choose a more difficult transmembrane apoplasmic pathway for the mode of phloem unloading during ripening? The apoplasmic unloading pathway seems linked to the property of fruit flesh to accumulate a high level of soluble sugars (Patrick, 1997; Zhang et al., 2004). As a matter of fact, the level of total soluble sugars in the phloem of pedicel of grape berry is lower than 50 mM, whereas it reaches more than 500 mM at the beginning of ripening and 1,000 mM at the late ripening stage in the cytosol/vacuole and approximately 200 mM in the apoplasmic space of berries (Fig. 4A). This high level of soluble sugars may result in a considerable rise in turgor pressure in PCs. If the SE-CC complex were symplasmically connected with the surrounding PCs via plasmodesmal channels, the high turgor pressure driven by the sugar accumulation in the storage parenchyma would impact on bulk flow through phloem by enhancing turgor pressure in the terminal release sieve tubes (Patrick, 1997). Breaking the symplasmic linkage separates turgor pressure of sieve tubes from

Figure 4. (*Continued*).
negative (−) numbers indicate the days before the onset of ripening, and the days after the onset of ripening are indicated by numbers 1 to 5. Arrows indicate the corresponding sampling time (at 4 and 2 d before the onset of ripening) of the columns of the immunoblotting data. C and D, Berries collected 6 d before the onset of ripening. C, Acid invertases visualized by immunogold particles were localized on cell walls between SE and CC and in the vacuole of CC. D, Acid invertases were shown to be numerous in the vacuole of PC with a lower density of the enzyme molecules on the cell wall between PCs. E and F, Berries collected 2 d after onset of ripening. E, Acid invertases on cell walls between SE and CC were shown to be much more numerous than those localized in the vacuole of CC. F, Acid invertases were predominantly localized on cell walls of PCs. Few acid invertase molecules were seen in vacuoles of PC. Bars = 1 μm. Abbreviations: cc, companion cell; cw, cell wall; pc, parenchyma cell; se, sieve element; v, vacuole. Each value presented in A and B is the mean of five replicates ± SD.

the surrounding ground tissues, which prevents dampening of the pressure difference between the import phloem in source leaves and the terminal release phloem in the sink berries, and hence ensures efficient long-distance phloem transport from source leaves to ripening berries. The elevated soluble sugar levels in the apoplasmic space of berries from the onset of ripening (Fig. 4A) may be favorable to the maintenance of this turgor pressure gradient through an osmo-regulatory mechanism (Patrick, 1997; van Bel, 2003). In addition, the conductivity of the berry xylem vessels was found to be also reduced from the time of onset of ripening (During et al., 1987; Findlay et al., 1987), which results in a hydraulic isolation of the berry xylem and contributes to the mechanism to prevent apoplasmic sugar flow from moving out of the berries. This may be a common feature in the terminal strong storage sinks accumulating high level of soluble sugars as shown in apple fruits (Zhang et al., 2004). In these sinks, setting up a mechanism for maintenance of driving force by the sinks is highly necessary, unlike vegetative sinks, such as vegetative apices, stems, roots, sink leaves, and potato tubers, and even reproductive developing seeds, where a symplasmic phloem unloading predominates (Patrick, 1997). Additionally, the predominantly apoplasmic unloading during the ripening process of grape berry requires an efficient mechanism for sugar transport across the membranes. The expression of two grape Suc transporters, VvSUT1 and VvSUC12, and two hexose transporters, VvHT1 and VvHT2, was shown to be up-regulated in berries from the onset of ripening (Davies et al., 1999; Fillion et al., 1999; Ageorges et al., 2000; Manning et al., 2001; Vignault et al., 2005), which potentially provides machinery to mediate this trans-membrane transport pathway of soluble sugars. Plasma membrane H^+-ATPase, which drives sugar transporters by generating the proton motive force across plasma membranes (Sondergaard et al., 2004), was shown to be activated by an abscisic acid-stimulated protein kinase that was up-regulated from the onset of ripening (Yu et al., 2006), supporting the occurrence of an enhanced capability of trans-membrane sugar transport from this time. The young growing grape berries during Stages I and II accumulate a level of soluble sugars comparable to or even lower than that in the phloem of pedicel (see Fig. 4), which may explain operation of the symplasmic phloem unloading pathway during these stages.

MATERIALS AND METHODS

Plant Material and Chemicals

Grape (*Vitis vinifera* × *Vitis labrusca* L. cv Kyoho) berries from 4- to 5-year-old plants were used for the experiments. The berries harvested at selected stages for assays of acid invertases were processed immediately or frozen in liquid nitrogen before being stored at −80°C. Goat anti-rabbit IgG antibody conjugated with 10 nm gold and goat anti-rabbit IgG antibody conjugated with alkaline phosphatase were purchased from Amersham Pharmacia Biotech. All other chemicals were purchased from Sigma, unless otherwise noted.

Tissue Preparation for Structural Observation

The sections prepared from the paraffin-embedded flesh tissue (see Fig. 1A for the sampling sites) were used for the observations of histological structure. The method described by Zhang et al. (2004) was used for the ultrastructural observations. Briefly, the glutaraldehyde and OsO_4 double-fixed tissues were embedded with Spurr for preparation of ultrathin sections. These sections (approximately 60–90 nm in thickness) were mounted on 100-mesh copper grids coated with 0.3% Formvar film for the ultrastructural observation with a JEM-100S transmission electron microscope.

Measurement of Plasmodesmal Density

The method for measurements of plasmodesmal density was adapted from Kempers et al. (1998) and used in our previous study (Zhang et al., 2004). Five group series of transverse ultrathin sections were prepared from the Spurr-infiltrated flesh samples, in which each group was cut at a distance of approximately 20 μm from the previous one. From each group, six pieces of ultrathin sections were picked at random and put on the copper grids of 100 meshes. Five scopes (each consisting of phloem and its surrounding PCs) were observed from each ultrathin section. Plasmodesmata were counted at all cell interfaces, i.e. the interfaces between SE/CC, SE/PC, CC/PC, and PC/PC (PC includes phloem parenchyma and flesh storage parenchyma) in each selected field. The results of the plasmodesmal counting were given as the number of plasmodesmata per micron of specific cell/cell interface length on transversal section, which is referred to as plasmodesmal density (no. plasmodesmata μm^{-1}).

CFDA and Texas Red Labeling

The CFDA labeling was done essentially as described previously (Zhang et al., 2004). Each berry was labeled with approximately 100 μL of 1 mg mL^{-1} CFDA aqueous solution (prepared from a stock solution in acetone). The CFDA solution was introduced into the berry from the axis of cluster or the pedicel (Fig. 1A) by a cotton thread immersed in a tube at one end and with the other end passing through the phloem zone of the pedicel. Berries were allowed to translocate the CF for 72 h. The treated berries were harvested at selected times and quickly taken to the laboratory with an ice bucket. The tissues were subsequently sectioned and examined by CLSM. Attempts to introduce CFDA into the berries from the leaves were conducted by the technique of Roberts et al. (1997). Whether CFDA was introduced from the cluster axis or pedicel or the leaf, the transport pathway in the berry tissue was the same, but the arrival of CF to the sampling site was observed from 3 to 4 h after cluster axis or pedicel loading, but from 16 to 17 h after leaf infiltration. These velocities were comparable to that of [^{14}C]Suc transport into the berry (see Fig. 2S). Furthermore, CF sometimes failed to be transferred into the berries after leaf infiltration, probably because of disconnection of vascular strands. Therefore, the cluster axis- and pedicel-CFDA loading method was chosen because of the high speed of transport and of its more reliable efficiency.

To allow the xylem tissue to be seen easily under the CLSM, the pedicel of the detached CFDA-treated berries was immersed in a solution containing 1 mg mL^{-1} of 3-kD Texas Red dextran (Molecular Probes) for half an hour before preparing the sections for examination under CLSM.

Labeling with a GFP-Tagged Viral Movement Protein

The fusion protein of the viral 3a MP:GFP (57 kD) and the dimeric GFP (GFP:GFP fusion as a control, 54 kD) were used to further trace the intercellular connections in berry tissues. The *CoYMV:3a MP:GFP* vector carries the DNA construct encoding the fusion protein of 3a MP of the *Cucumber mosaic virus* and GFP tag under the control of the CC-specific promoter of CoYMV (Itaya et al., 2002; Matsuda et al., 2002). The *CoYMV:GFP:GFP* vector carries the DNA construct encoding the dimeric GFP fusion protein under the control of the same CoYMV (Itaya et al., 2002). Both vectors were generously provided by Dr. Biao Ding (Department of Plant Biology and Plant Biotechnology Center, Ohio State University, Columbus, Ohio). Each plasmid was used to transform *Agrobacterium tumefaciens* (LBA4404), as described previously (Itaya et al., 1998). An Agrobacterium-mediated leaf disc transformation method, used by Itaya et al. (2002), was adapted to generate transgenic berry tissues. Briefly,

berry discs of 1 to 2 mm in thickness were prepared from sterilized grape berry, incubated for 10 min with *A. tumefaciens* LBA4404 strain containing the 3a MP:GFP or dimeric GFP plasmid, and then the tissues were placed on filter paper soaked with Murashige and Skoog medium under aseptic growth conditions in the dark. Twelve hours later, fluorescence of GFP in the treated discs or the sections prepared from the treated discs was observed under CLSM at intervals of 1 to 2 h. To ensure that the observed tissues were in vivo functional, protoplasts were prepared from these tissues, and the viability of the protoplasts was checked using the fluorescein diacetate-propidium iodide double-staining technique essentially as described previously (Jones and Senft, 1985; Zhang et al., 2001a). The investigations showed that more than 95% of the protoplasts were alive, and, thus, the tissues were fully in vivo functional.

Tissue Sectioning and Microscopy

Prior to CLSM, the phloem zone of the tissue was carefully cut by free hand or by a freezing microtome (Frigocut-2700; Leica) into transverse or longitudinal sections that were immersed immediately into 80% (v/v) glycerol to prevent dye loss (for long time preservation, the immersion oil was used).

A Zeiss LSM 510 confocal laser scanning microscope was used to image CF, 3a MP:GFP, and Texas Red dextran transport. CF or GFP was excited by the 488-nm beam produced by a 25-mW Krypton/Argon laser. On occasions where detached berries were allowed to transpire Texas red dextran after CF import, the sections were imaged first for CF by using blue (488 nm) light and immediately afterward for Texas Red dextran by using green excitation (568 nm) light (Roberts et al., 1997). The images taken at the different wavelengths were then superimposed to reveal phloem and xylem transport on a single image of the section.

An Olympus BH2 fluorescence microscope was used to image CF transport in whole grape berry. Fresh hand-free sections of whole berry at selected sampling sites (see Fig. 3), stained with 80% (v/v) glycerol, were examined under a blue excitation filter.

Immunogold Labeling

Specimen preparation and immunogold labeling were conducted essentially according to Zhang et al. (2001b). Briefly, the ultrathin sections prepared as described above for ultrastructural observation from Spurr-embedded berry tissues in the peripheral carpellary bundle zone (Fig. 1A) were incubated first with rabbit antiserum directed against either soluble or cell wall acid invertase of the apple (*Malus domestica*) fruit prepared in our laboratory (Pan et al., 2005a, 2005b), and then with secondary antibody (goat anti-rabbit IgG antibody conjugated with 10 nm gold). The sections were finally double-stained with uranyl acetate and alkaline lead citrate and examined with a JEM-100S electron microscope.

The specificity and reliability of the immunogold labeling were tested by two negative controls. In the first one, the antiserum was omitted to test possible unspecific labeling of the goat anti-rabbit IgG antibody-gold conjugate. In the second one, rabbit preimmune serum was used instead of the rabbit antiserum before immunogold labeling to test the specificity of the antiserum. More than three repetitions of the control experiments were conducted for each sample.

Enzyme Assay, SDS-PAGE, and Immunoblotting

The enzyme exaction and assays of soluble or cell wall acid invertase activity were done essentially as described previously (Pan et al., 2005b). Briefly, the extracting buffer A medium was composed of 150 mM Tris-HCl, pH 8.0, 2 mM ethylenediamine tetraacetic acid, 10 mM $MgCl_2$, 0.2% (v/v) 2-mercaptoethanol, 0.1 mM phenylmethyl sulfonyl fluoride, 1 mM benzamidine, 10 mM ascorbic acid, and 3% (w/v) polyvinylpolypyrrolidone. The slurry was passed through four layers of cheesecloth. The filtrate was centrifuged at 16,000*g* for 20 min and the supernatant was used for the assays of the SAI. The residue, which was used for the preparation of cell wall-bound invertase (CWI), was rinsed with the same buffer without polyvinylpolypyrrolidone until the effluent was free of proteins. From this material, CWI was extracted in buffer A supplemented with 0.5 M NaCl with gentle shaking for 24 h. After centrifugation, the supernatant was used for the enzyme assays of CWI. All the extracting procedures were carried out at 4°C. Acid invertase activities were assayed in the soluble and insoluble fractions in 0.3 mL of 100 mM sodium acetate buffer, pH 4.8, 0.1 mL of 100 mM Suc, and 0.1 mL enzyme sample, as described by Schaffer et al. (1987). The reducing sugars produced were determined with the 3,5-dinitrosalicylic acid-based method according to Miller (1959).

The enzyme exaction and assays of Suc synthase activity were done as described by Huber and Akazawa (1986), with modifications. Briefly, the above-described extracting buffer A was used to prepare the crude extracts for the enzyme assays except the pH of the medium that was adjusted to 7.5. The enzymatic activity in the Suc cleavage direction was assayed, at 30°C, in the presence of 100 mM Suc, using an enzyme-coupling method based on UDP-dependent formation of hexose sugars from Suc.

SDS-PAGE and immunoblotting of the enzyme extracts were conducted according to Pan et al. (2005b). Briefly, after electrophoretic transfer from the polyacrylamide gels, the nitrocellulose membranes were blocked and incubated overnight at 4°C in the antiserum directed against either soluble or cell wall acid invertase of the apple fruit prepared in our laboratory (Pan et al., 2005a, 2005b). Following extensive washes, the membranes were incubated with goat anti-rabbit IgG-alkaline phosphatase conjugate. The membranes were stained with 5-bromo-4-chloro-3-indolyl phosphate and nitro blue tetrazolium.

Protein concentrations were determined by the method of Bradford (1976) with bovine serum albumin as a standard.

$^{14}CO_2$ Labeling and Autoradiography

The $^{14}CO_2$ labeling and autoradiography were done as described previously (Zhang et al., 2004).The leaves located near the grape clusters were labeled with $^{14}CO_2$ to follow subsequent movement of radioactivity into berries. The leaves were enclosed in plastic bags, and the radiolabel was injected into a vial inside the bag. Each shoot received 1.85 MBq of $^{14}CO_2$ released from [^{14}C]bicarbonate by addition of excess 3 M lactic acid. The leaves were exposed to $^{14}CO_2$ for 1 h before injecting excess 3 M KOH to neutralize the acid and to absorb any remaining $^{14}CO_2$. After labeling, the shoots were left for 18 h to translocate ^{14}C to fruits.

After $^{14}CO_2$ labeling, berry tissue for autoradiography was selected and sectioned before rapid freezing in liquid nitrogen between sheets of paper. The frozen sample was gently compressed between aluminum plates and freeze-dried. After drying, the tissue was pressed flat and autoradiographed using Kodak BioMax MR-1 film at −80°C for 5 d.

Soluble Sugar Determination

Briefly, the frozen powders of berries were homogenized at 0°C. The sugars in the supernatants of the homogenates after centrifugation were separated by HPLC and detected by the pulsed amperometric method (Hardy et al., 1988). Suc, Glc, and Fru were identified according to their retention times, and quantified in relation to sugar standards.

Collection and Analysis of Phloem Exudates

Phloem exudates were collected from pedicel using the method described by Chen et al. (2001). The pedicel was cut under water and subsequently rinsed to avoid contamination of cellular fluid. Each pedicel was then incubated in 300 μL of 15 mM EDTA solution, pH 7.5, for 4 h in a humid chamber at 20°C. Phloem exudates were lyophilized and stored at −80°C. The samples were analyzed for soluble sugars by HPLC as described above.

Collection and Analysis of Apoplastic Sap

Apoplastic sap was collected from freshly harvested grape clusters essentially as described by Ruan et al. (1995) and Beruter and Studer Feusi (1995), using a pressure dehydration procedure with a Scholander pressure chamber (Scholander et al., 1965). By increasing the external air pressure on the cluster, xylem sap was expelled from the peduncle of the cluster when the pressure was the same as the water potential of the cluster. The pressure was further increased by 4 bars and the exudates from the peduncle were collected in a pipette during a 2-h period. The collected exudates were analyzed for soluble sugars by HPLC as described above.

ACKNOWLEDGMENTS

We thank Dr. Biao Ding (Ohio State University, Columbus, Ohio) for his generous gift of the CoYMV:3a MP:GFP and CoYMV:GFP:GFP vectors, and

Prof. Xue-Chen Wang (China Agricultural University, Beijing) for his advice in plant transformation.

Received April 3, 2006; accepted July 15, 2006; published July 21, 2006.

LITERATURE CITED

Ageorges A, Issaly N, Picaud S, Delrot S, Romieu C (2000) Identification and functional expression in yeast of a grape berry sucrose carrier. Plant Physiol Biochem **38:** 177–185

Beruter J, Studer Feusi ME (1995) Comparison of sorbitol transport in excised tissue discs and cortex tissue of intact apple fruit. J Plant Physiol **146:** 95–102

Bradford MM (1976) A rapid and sensitive method for the quantitation of microgram quantities of protein utilizing the principle of protein-dye binding. Anal Biochem **72:** 248–254

Brown SC, Coombe BG (1985) Solute accumulation by grape pericarp cells. III. Sugar changes in vivo and the effect of shading. Biochem Physiol Pflanz **180:** 371–381

Chen S, Petersen BL, Olsen CE, Schulz A, Halkier BA (2001) Long-distance phloem transport of glucosinolates in Arabidopsis. Plant Physiol **127:** 194–201

Coombe B (1992) Research on development and ripening of grape berry. Am J Enol Vitic **43:** 101–111

Davies C, Robinson SP (1996) Sugar accumulation in grape berries. Cloning of two putative vacuolar invertase cDNAs and their expression in grapevine tissues. Plant Physiol **111:** 275–283

Davies C, Wolf T, Robinson SP (1999) Three putative sucrose transporters are differentially expressed in grapevine tissues. Plant Sci **147:** 93–100

During H, Lang A, Oggionni F (1987) Patterns of water flow in Riesling berries in relation to developmental changes in their xylem morphology. Vitis **26:** 123–131

Fillion L, Ageorges A, Picaud S, Coutos-Thevenot P, Lemoine R, Romieu C, Delrot S (1999) Cloning and expression of a hexose transporter gene expressed during the ripening of grape berry. Plant Physiol **120:** 1083–1093

Findlay N, Oliver KJ, Nu N, Coombe BG (1987) Solute accumulation by grape pericarp cells. IV. Perfusion of grape pericarp apoplast via the pedicel and evidence for xylem malfunction in ripening berries. J Exp Bot **38:** 668–679

Fisher DB, Oparka KJ (1996) Post-phloem transport: principles and problems. J Exp Bot **47:** 1141–1154

Frommer WB, Sonnewald U (1995) Molecular analysis of carbon partitioning in solanaceous species. J Exp Bot **46:** 587–607

Gisel A, Barella S, Hempel FD, Zambryski PC (1999) Temporal and spatial regulation of symplastic trafficking during development in *Arabidopsis thaliana* apices. Development **126:** 1879–1889

Gisel A, Hempel FD, Barella S, Zambrysky PC (2002) Leaf-to-shoot apex movement of symplastic tracer is restricted coincident with flowering in Arabidopsis. Proc Natl Acad Sci USA **99:** 1713–1717

Hardy MR, Townsend RR, Lee YC (1988) Monosaccharide analysis of glycol-conjugates by anion exchange chromatography with pulsed amperometric detection. Anal Biochem **170:** 54–62

Haupt S, Duncan GH, Holzberg S, Oparka KJ (2001) Evidence for symplastic phloem unloading in sink leaves of barley. Plant Physiol **125:** 209–218

Huber SC, Akazawa T (1986) A novel sucrose synthase pathway for sucrose degradation in cultured sycamore cells. Plant Physiol **81:** 1008–1013

Imlau A, Truenit E, Sauer N (1999) Cell-to-cell and long-distance trafficking of the green fluorescent protein in the phloem and symplastic unloading of the protein into sink tissue. Plant Cell **11:** 309–322

Itaya A, Ma F, Qi Y, Matsuda Y, Zhu Y, Liang G, Ding B (2002) Plasmodesma-mediated selective protein traffic between ''symplasmically isolated'' cells probed by a viral movement protein. Plant Cell **14:** 2071–2083

Itaya A, Woo YM, Masuta C, Bao Y, Nelson RS, Ding B (1998) Developmental regulation of intercellular protein trafficking through plasmodesmata in tobacco leaf epidermis. Plant Physiol **118:** 373–385

Jones KH, Senft JA (1985) An improved method to determine cell viability by simultaneous staining with fluorescein diacetate-propidium iodide. J Histochem Cytochem **33:** 77–79

Kempers R, Ammerlaan A, van Bel AJE (1998) Symplasmic constriction and ultrastructural features of sieve element/companion cell complex in the transport phloem of apoplasmically and symplasmically phloem-loading species. Plant Physiol **116:** 271–278

Kim I, Hempel FD, Sha K, Pfluger J, Zambryski PC (2002) Identification of a developmental transition in plasmodesmatal function during embryogenesis in Arabidopsis thaliana. Development **129:** 1261–1272

Koch KE, Avigne WT (1990) Post-phloem, nonvascular transfer in citrus: kinetics, metabolism, and sugar gradients. Plant Physiol **93:** 1405–1416

Manning K, Davies C, Bowen HC, White PJ (2001) Functional characterization of two ripening-related sucrose transporters from grape berries. Ann Bot (Lond) **87:** 125–129

Matsuda Y, Liang G, Zhu Y, Ma F, Nelson RS, Ding B (2002) The Commelina yellow mottle virus promoter drives companion-cell-specific gene expression in multiple organs of transgenic tobacco. Protoplasma **220:** 51–58

Miller GL (1959) Use of dinitrosalicylic acid reagent for determination of reducing sugars. Anal Chem **31:** 426–428

Oparka KJ (1990) What is phloem unloading? Plant Physiol **94:** 393–396

Oparka KJ, Roberts AG, Boevink P, Cruz SS, Roberts I, Pradel KS, Imlau A, Kotlizky G, Sauer N, Epel B (1999) Simple, but not branched, plasmodesmata allow the nonspecific trafficking of proteins in developing tobacco leaves. Cell **97:** 743–754

Oparka KJ, Santa Cruz S (2000) The great escape: phloem transport and unloading of macromolecules. Annu Rev Plant Physiol Plant Mol Biol **51:** 323–347

Oparka KJ, Turgeon R (1999) Sieve elements and companion cells—traffic control centers of the phloem. Plant Cell **11:** 739–750

Pan QH, Zou KQ, Peng CC, Wang XL, Zhang DP (2005a) Purification, biochemical and immunological characterization of acid invertases from apple fruit. J Integr Plant Biol **47:** 50–59

Pan QH, Li MJ, Peng CC, Zhang N, Zou X, Zou KQ, Wang XL, Yu XC, Wang XF, Zhang DP (2005b) Abscisic acid activates acid invertases in developing grape berry. Physiol Plant **125:** 157–170

Patrick JW (1997) Phloem unloading: sieve element unloading and post-sieve element transport. Annu Rev Plant Physiol Plant Mol Biol **48:** 191–222

Patrick JW, Offler CE (1996) Post-sieve element transport of photoassimilates in sink regions. J Exp Bot **47:** 1165–1177

Quick WP, Schaffer AA (1996) Sucrose metabolism in sources and sinks. *In* E Zamski, AA Schaffer, eds, Photoassimilate Distribution in Plants and Crops: Source-Sink Relationships. Marcel Dekker, New York, pp 115–156

Roberts AG, Santa Cruz S, Roberts IM, Prior DAM, Turgeon R, Oparka KJ (1997) Phloem unloading in sink leaves of *Nicotiana benthamiana*: comparison of a fluorescent solute with a fluorescent virus. Plant Cell **9:** 1381–1396

Ruan YL, Llewellyn DJ, Furbank RT (2001) The control of single-celled cotton fiber elongation by developmentally reversible gating of plasmodesmata and coordinated expression of sucrose and K+ transporters and expansin. Plant Cell **13:** 47–60

Ruan YL, Mate C, Patrick JW, Brady CJ (1995) Non-destructive collection of apoplast fluid from developing tomato fruit using a pressure dehydration procedure. Aust J Plant Physiol **22:** 761–769

Ruan YL, Patrick JW (1995) The cellular pathway of post-phloem sugar transport in developing tomato fruit. Planta **196:** 434–444

Ruan YL, Xu SM, White R, Furbank RT (2004) Genomic and developmental evidence for the role of plasmodesmal regulation in cotton fiber elongation mediated by callose turnover. Plant Physiol **136:** 4104–4113

Schaffer AA, Sagee O, Goldschmidt EE, Goren R (1987) Invertase and sucrose synthase activity, carbohydrate status and endogenous IAA levels during citrus leaf development. Physiol Plant **69:** 151–155

Scholander PF, Hammel HT, Bradstreet ED, Hemmingsen EA (1965) Sap pressure in vascular plants. Science **148:** 339–346

Sondergaard TE, Schulz A, Palmgren MG (2004) Energization of transport process in plants. Roles of plasma membrane H^+-ATPase. Plant Physiol **136:** 2475–2482

van Bel AJE (2003) The phloem, a miracle of ingenuity. Plant Cell Environ **26:** 125–149

Vignault C, Vachaud M, Cakir B, Glissant D, Dedaldechamp F, Buttner M, Atanassova R, Fleurat-Lessard P, Lemoine R, Delrot S (2005) *VvHT1* encodes a monosaccharide transporter expressed in the conducting complex of the grape berry phloem. J Exp Bot **56:** 1409–1418

Viola R, Roberts AG, Haupt S, Gazzani S, Hancock RD, Marmiroli N, Machray GC, Oparka KJ (2001) Tuberization in potato involves a switch from apoplastic to symplastic phloem unloading. Plant Cell **13:** 385–398

Xia GH, Zhang DP (2000) Intercellular symplasmic connection and isolation of unloading zone in flesh of the developing grape berry. Acta Bot Sin **42:** 898–904

Yu XC, Li MJ, Gao GF, Feng HZ, Geng XQ, Peng CC, Zhu SY, Wang XJ, Shen YY, Zhang DP (2006) Abscisic acid stimulates a calcium-dependent protein kinase in grape berry. Plant Physiol **140:** 558–576

Zhang DP, He FL, Jia WS (2001a) Cell biological mechanism for triggering of ABA accumulation under water stress in *Vicia faba* leaves. Sci China Ser C Life Sci **44:** 421–428

Zhang DP, Lu YM, Wang YZ, Duan CQ, Yan HY (2001b) Acid invertase is predominantly localized to cell walls of both the practically symplasmically isolated element/companion cell complex and parenchyma cells in developing apple fruits. Plant Cell Environ **24:** 691–702

Zhang LY, Peng YB, Pelleschi-Travier S, Fan Y, Lu YF, Lu YM, Gao XP, Shen YY, Delrot S, Zhang DP (2004) Evidence for apoplasmic phloem unloading in developing apple fruit. Plant Physiol **135:** 574–586